Article

Immunity

Sequential Activation of Two Pathogen-Sensing Pathways Required for Type I Interferon Expression and Resistance to an Acute DNA Virus Infection

Highlights

- TLR9, MyD88, STING, and IRF7 are required for IFN-I expression in the dLN
- Inflammatory monocytes are the major producers of IFN-I in the dLN
- TLR9, MyD88, and IRF7 are required in $CD11c^+$ cells for iMo recruitment to dLNs
- STING-IRF7 are required in iMos for IFN-α and STING-NF-κB for IFN-β expression in iMos

Authors

Ren-Huan Xu, Eric B. Wong, Daniel Rubio, ..., Shinu John, Mark Shlomchik, Luis J. Sigal

Correspondence

luis.sigal@jefferson.edu

In Brief

How different pathogen-sensing mechanisms contribute to the expression of IFN-I in vivo is unclear. Sigal and colleagues report that in lymph nodes of ectromelia-virus-infected mice, $CD11c^+$ cells use TLR9-MyD88-IRF7 to recruit inflammatory monocytes (iMos). In turn, infected iMos express IFN-α and IFN-β through STING-IRF7 and STING-NF-κB, respectively.

Xu et al., 2015, Immunity *43*, 1148–1159
December 15, 2015
http://dx.doi.org/10.1016/j.immuni.2015.11.015

CellPress

CellPress

Immunity
Article

Sequential Activation of Two Pathogen-Sensing Pathways Required for Type I Interferon Expression and Resistance to an Acute DNA Virus Infection

Ren-Huan Xu,[1,5] Eric B. Wong,[1,6] Daniel Rubio,[1,7] Felicia Roscoe,[1] Xueying Ma,[1] Savita Nair,[1] Sanda Remakus,[1] Reto Schwendener,[2] Shinu John,[3] Mark Shlomchik,[4] and Luis J. Sigal[1,6,*]

[1]Immune Cell Development and Host Defense Program, The Research Institute at Fox Chase Cancer Center, 333 Cottman Avenue, Philadelphia, PA 19111, USA

[2]Institute of Molecular Cancer Research, University Zurich, 8057 Zurich, Switzerland

[3]Department of Laboratory Medicine, Yale University, New Haven, CT 06520, USA

[4]Department of Immunology, University of Pittsburgh School of Medicine, 200 Lothrop Street, Pittsburgh, PA 15261, USA

[5]Present address: Novavax Inc., 20 Firstfield Road, Gaithersburg, MD 20878, USA

[6]Present address: Department of Microbiology and Immunology, Thomas Jefferson University, BLSB 730, 233 South 10th Street, Philadelphia, PA 19107, USA

[7]Present address: GlaxoSmithKline, 709 Swedeland Road, King of Prussia, PA 19406, USA

*Correspondence: luis.sigal@jefferson.edu

http://dx.doi.org/10.1016/j.immuni.2015.11.015

SUMMARY

Toll-like receptor 9 (TLR9), its adaptor MyD88, the downstream transcription factor interferon regulatory factor 7 (IRF7), and type I interferons (IFN-I) are all required for resistance to infection with ectromelia virus (ECTV). However, it is not known how or in which cells these effectors function to promote survival. Here, we showed that after infection with ECTV, the TLR9-MyD88-IRF7 pathway was necessary in CD11c$^+$ cells for the expression of proinflammatory cytokines and the recruitment of inflammatory monocytes (iMos) to the draining lymph node (dLN). In the dLN, the major producers of IFN-I were infected iMos, which used the DNA sensor-adaptor STING to activate IRF7 and nuclear factor κB (NF-κB) signaling to induce the expression of IFN-α and IFN-β, respectively. Thus, in vivo, two pathways of DNA pathogen sensing act sequentially in two distinct cell types to orchestrate resistance to a viral disease.

INTRODUCTION

The ability of the innate immune system to sense infection is essential to mount innate and adaptive immune responses (Iwasaki and Medzhitov, 2010; Wu and Chen, 2014). It is well established that pathogen recognition receptors (PRRs) recognize pathogen-associated molecular patterns (PAMPs) to activate innate immune signaling pathways (Iwasaki and Medzhitov, 2010). PAMPs are typically microbial nucleic acids and other macromolecules with repetitive structures common to pathogens but not usually encountered in uninfected cells (Schenten and Medzhitov, 2011). PRR-initiated signaling cascades after virus infection culminate in the expression of type I interferon (IFN-I), pro-inflammatory cytokines, and chemokines that recruit and activate innate and adaptive immune cells (Wu and Chen, 2014).

PAMPs in the cell microenvironment are recognized by transmembrane PRRs that reside in the plasma and endosomal membranes, such as Toll-like receptors (TLRs)—for example, TLR9 recognizes double-stranded DNA in endosomes (Ahmad-Nejad et al., 2002; Hemmi et al., 2000). PAMPs in the cytosol, on the other hand, are sensed by cytosolic PRRs—for instance, RIG-I-like receptors (RLRs) detect cytosolic viral RNA species (Goubau et al., 2013; Vabret and Blander, 2013), whereas DNA-dependent activator of IFN-regulatory factors (DAI), interferon-activated gene 204 (Ifi204, IFI16 in humans), and cyclic-GMP-AMP (cGAMP) synthase (cGAS, encoded by *M21d1*) respond to cytosolic DNA (Wu and Chen, 2014).

To signal, PRRs use adapters. The adapters for TLRs are MyD88 and TIR-domain-containing adaptor-inducing IFN-β (TRIF); for RLRs, mitochondrial antiviral-signaling protein (MAVS); and for DNA-sensing PRRs, STING (Wu and Chen, 2014). Additional signaling steps downstream of these adapters link PRRs to the activation of several transcription factors, most frequently IRF3, IRF7, and NF-κB. These transcription factors induce the expression of IFN-I and pro-inflammatory cytokines (Wu and Chen, 2014).

Soon after breaching epithelia, many pathogenic viruses rapidly spread through afferent lymphatics to the regional draining lymph nodes (dLNs), from where they disseminate through efferent lymphatics to the bloodstream, ultimately reaching their target organs (Flint et al., 2009; Virgin, 2007). Ectromelia virus, an Orthopoxvirus (a genus of large DNA viruses), is the causative agent of mousepox, the mouse homolog of human smallpox (Esteban and Buller, 2005). After infection through the skin of the footpad, ECTV spreads lympho-hematogenously to cause systemic disease. Indeed, ECTV was the virus used to describe this form of dissemination (Fenner, 1948) and is used as the textbook paradigm of lympho-hematogenous spread (Flint et al., 2009; Virgin, 2007).

During lympho-hematogenous dissemination, a swift anti-viral innate response in the dLN can play a major role in restricting

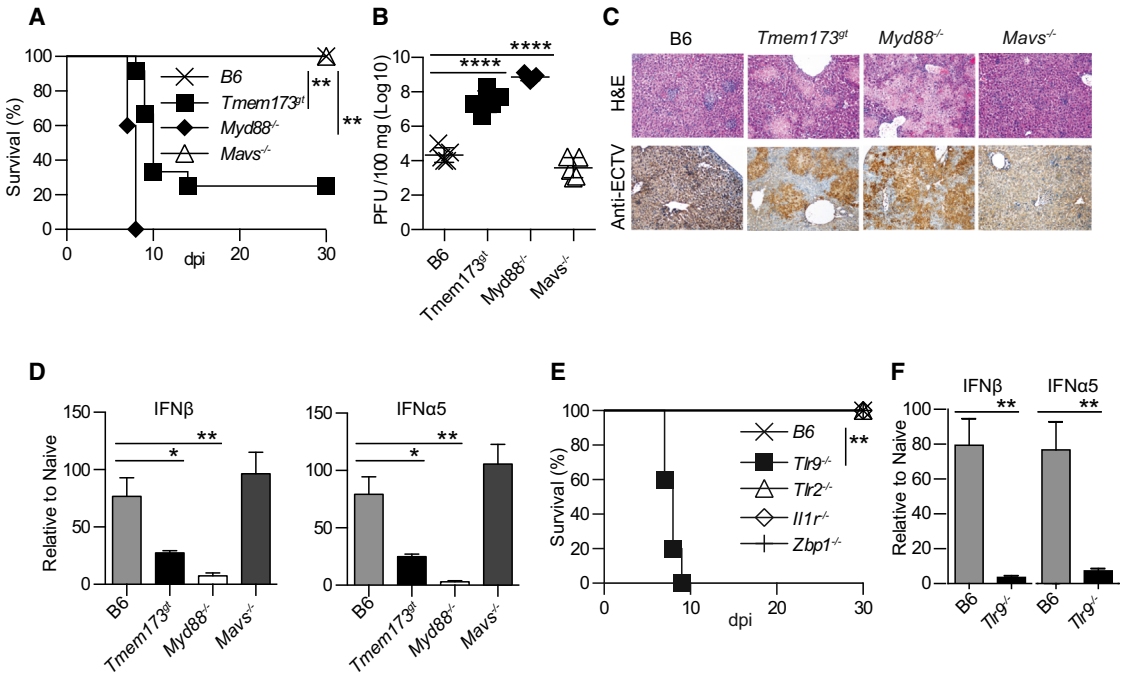

Figure 1. TLR9, MyD88, and STING Are Critical for Resistance to Mousepox and the Efficient Induction of IFN-I in Lymph Nodes

Mice were infected with 3,000 PFUs of ECTV in the footpad.

(A) Survival of the indicated mice.

(B) Virus loads in the livers of the indicated mice at 7 dpi as determined by plaque assay.

(C) Liver sections of the indicated mice at 7 dpi stained with H&E (top) or immunostained with anti-ECTV Ab (bottom).

(D) Expression of IFN-I in the dLNs of the indicated mice at 2.5 dpi as determined by RT-qPCR.

(E) Survival of the indicated mice.

(F) Expression of IFN-I in the dLNs of the indicated mice at 2.5 dpi as determined by RT-qPCR.

Data are shown either as individual mice with mean ± SEM or as mean ± SEM. Each panel displays data from one experiment with five mice per group and is representative of three similar experiments. For all, *$p < 0.05$; **$p < 0.01$; ***$p < 0.001$; ****$p < 0.0001$.

viral spread and deterring disease (Fang et al., 2008; Junt et al., 2007; Kastenmüller et al., 2012). It is therefore important to understand how different mechanisms of virus sensing contribute to this process. Here we dissect the contribution of PRRs to the antiviral response to ECTV in the dLN. We show that the TLR9-MyD88-IRF7 axis is necessary in $CD11c^+$ cells for the chemokine-driven recruitment of inflammatory monocytes (iMos) to the dLN, but not directly essential for IFN-I production. Once iMos are infected, they use STING-IRF7 and STING-NF-κB pathways to induce the expression of IFN-α and IFN-β, respectively. Collectively, our work shows that the TLR9-MyD88-IRF7 and STING-IRF7 or STING-NF-κB pathways have non-redundant, complementary, and sequential roles in IFN-I expression in the dLNs and in resistance to a highly pathogenic viral disease.

RESULTS

TLR9-MyD88 and STING Are Critical for Resistance to Mousepox and the Efficient Induction of IFN-I in Lymph Nodes

The TLR adaptor MyD88 is required for the inherent resistance of B6 mice to mousepox (Rubio et al., 2013; Sutherland et al., 2011), whereas TRIF is not necessary (data not shown). We performed experiments to identify the specific role of MyD88, as well as of MAVS- and STING-driven pathways, in resistance to mousepox and IFN-I expression in vivo during acute ECTV infection. We found that after infection with ECTV in the footpad, mice deficient in MyD88 ($Myd88^{-/-}$) or with inactive STING ($Tmem173^{gt}$), but not those lacking MAVS ($Mavs^{-/-}$), were susceptible to lethal mousepox (Figure 1A). Nevertheless, death occurred in 100% of $Myd88^{-/-}$ but in only 80% $Tmem173^{gt}$ mice, a difference that was reproducible and highly significant ($p < 0.0001$) suggesting a more profound impairment in the absence of MyD88 than in the absence of STING signaling. Consistently, virus loads (Figure 1B) and pathology (Figure 1C) in the livers of $Myd88^{-/-}$ and $Tmem173^{gt}$, but not of $Mavs^{-/-}$, mice were significantly higher than in B6 mice. Notably, the virus titers were significantly lower ($p < 0.01$) and the liver pathology was somewhat milder in $Tmem173^{gt}$ than in $Myd88^{-/-}$ mice. We next performed reverse transcriptase quantitative polymerase chain reaction (RT-qPCR) on RNA obtained from the dLNs at 2.5 days post infection (dpi). We found that $Myd88^{-/-}$ and $Tmem173^{gt}$ but not $Mavs^{-/-}$ mice expressed significantly lower levels of "early" IFN-β and "late" IFN-α5 than B6 mice. However, $Myd88^{-/-}$ mice expressed significantly lower levels of IFN-β ($p < 0.0001$) and IFN-α5 ($p < 0.0001$) than $Tmem173^{gt}$ mice (Figure 1D). Thus, MyD88 and STING, but not MAVS, are both critical adapters for resistance to lethal ECTV infection and the efficient

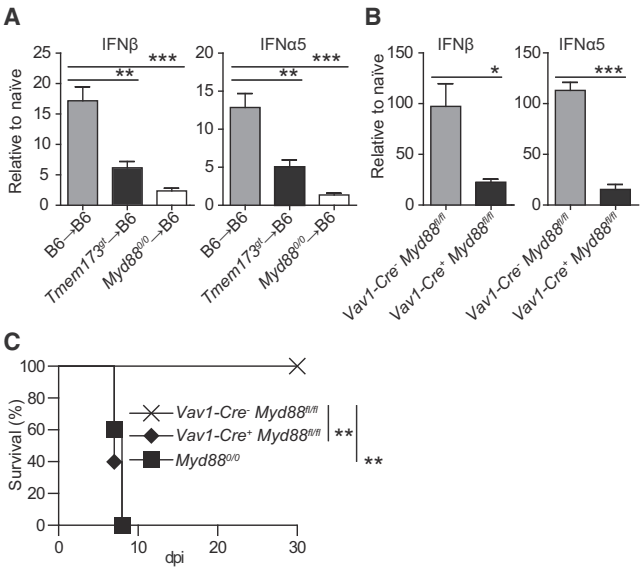

Figure 2. IFN-I Expression Requires MyD88 and STING in Bone-Marrow-Derived Cells

Mice were infected with 3,000 PFUs of ECTV in the footpad.

(A) Expression of IFN-I in the dLNs of the indicated bone marrow chimeras at 2.5 dpi.

(B) Expression of IFN-I in the dLNs of the indicated mice at 2.5 dpi. p values are compared to *Vav1*-Cre- *Myd88*$^{fl/fl}$.

(C) Survival of indicated mice.

When applicable, data are shown as mean ± SEM. Each panel displays data from one experiment with five mice per group and is representative of three similar experiments except for (A), which was performed twice. For all, *p < 0.05; **p < 0.01; ***p < 0.001; ****p < 0.0001.

expression of IFN-I in the dLNs in vivo. However, mice are significantly more susceptible to mousepox with absent *MyD88* than with deficient STING.

Next, we investigated several molecules upstream of MyD88 and STING that could be required for resistance to mousepox and/or IFN-I expression in the dLNs. As before, mice deficient in TLR9 (*Tlr9*$^{-/-}$), but not in other TLRs, were susceptible to mousepox (Rubio et al., 2013; Samuelsson et al., 2008; Sutherland et al., 2011). In contrast, mice deficient in the IL-1 receptor (*Il1r*$^{-/-}$), which also uses MyD88 as its adaptor (Muzio et al., 1997), and mice deficient in the cytosolic DNA sensor DAI (*Zbp1*$^{-/-}$) (Ishii et al., 2008), which is thought to signal through STING, were resistant (Figure 1E and not shown). Moreover, at 2.5 dpi, mice deficient in TLR9, but not in TLR2, IL-1R, or DAI, expressed significantly lower IFN-I in the dLNs than B6 mice (Figure 1F and not shown). Thus, among those we tested, the only PRR upstream of MyD88 that is required for IFN-I expression in the dLNs during ECTV infection is TLR9. Further, DAI is not the critical sensor for STING.

IFN-I Expression Requires MyD88 and STING in Bone-Marrow-Derived Cells

Next, we sought to identify the cells that produce IFN-I during infection. To distinguish the role of bone-marrow-derived versus parenchymal cells, we used bone marrow chimeras. Expression of IFN-β and IFN-α5 in the dLNs at 2.5 dpi was significantly lower in *Myd88*$^{-/-}$→B6 and *Tmem173*^{gt}→B6 than in B6→B6 chimeras. Expression of IFN-β and IFN-α5 was also significantly lower ($p < 0.05$ for IFN-β and $p < 0.01$ for IFN-α5) in *Myd88*$^{-/-}$→B6 than in *Tmem173*^{gt}→B6 chimeras (Figure 2A). In another approach, *Vav1*-Cre^{+} *Myd88*$^{fl/fl}$ mice, which specifically lack MyD88 in hematopoietic cells, expressed significantly less IFN-I than *Vav1*-Cre^{-} *Myd88*$^{fl/fl}$ controls (Figure 2B). Moreover, *Vav1*-Cre^{+} *Myd88*$^{fl/fl}$ but not *Vav1*-Cre^{-} *Myd88*$^{fl/fl}$ mice succumbed to mousepox with similar kinetics to constitutive *Myd88*$^{-/-}$ mice (Figure 2C). Consequently, both MyD88 and STING in bone-marrow-derived cells are essential for the efficient expression of IFN-I during ECTV infection in vivo. Moreover, MyD88 in hematopoietic cells is essential for resistance to mousepox.

Infected Inflammatory Monocytes Are Responsible for Most of the IFN-I Expressed in the dLNs

In several infection models, plasmacytoid dendritic cells (pDCs) sense infection through TLR9-MyD88 to become the major producers of IFN-I (Colonna et al., 2004; Ito et al., 2005). However, B6 mice depleted of pDCs with the anti-BST2 mAb 927 (Figure S1A; Blasius et al., 2006) did not differ significantly from mice treated with control rat IgG in terms of IFN-I expression in the dLNs at 2.5 dpi (Figure S1B) and of virus loads in the liver at 7 dpi (Figure S1C). Consistent with these findings, they did not show any differences in IFN-I expression in the dLNs at 5 dpi and were resistant to lethal mousepox (not shown). Hence, pDCs are neither the major producers of IFN-I in the dLNs nor essential for the resistance of B6 mice to mousepox after infection with ECTV.

Having found that pDCs are not the major producers of IFN-I in the dLNs, we attempted to identify the relevant bone-marrow-derived cells. In initial experiments analyzing the response to ECTV in the dLNs at 2.5 dpi, we found an increase in CD11b^{+} cells that also stained with the anti-Ly6C+G mAb Gr1 (Figure 3A, gate 1) but at lower levels than typical neutrophils (Figure 3A, gate 2). The absolute number of gate 1 cells peaked in the dLNs at 3 dpi (Figure 3B). At 5 dpi they had disappeared, most likely because at this time after infection the dLNs were almost acellular (not shown). The cells in gate 1 stained with anti-Ly6C but not anti-Ly6G mAbs (Figure 3C) and were mononuclear (Figure 3D), indicating that they were not neutrophils. These cells were MHC II^{+} and CD11c^{+} and expressed the monocyte or macrophage markers CD64 and F4/80 (Gautier et al., 2012) but were negative or low for the DC core markers CD26, CD117 (c-Kit), CD135 (Flt3), and BTLA (Figure 3E; Miller et al., 2012), suggesting that they were inflammatory monocytes (iMos) and not dendritic cells (DCs). Hereafter, we will refer to the cells in gate 1 as iMos.

Using ECTV-EGFP (Fang et al., 2008), we found that in the dLNs, ECTV preferentially infected myeloid and B cells (Figure S2), which are mostly MHC II^{+}. To identify the cell types that produce IFN-I in the dLNs, we determined IFN-I expression in sorted cell populations from the dLNs at 2.5 dpi. We found that IFN-I expression segregated with MHC II^{+} cells and, among these cells, iMos but not B cells expressed IFN-I (Figure 3F). We also sorted iMos, B cells, and the rest of the cells in the dLNs of ECTV-infected mice at 2.5 dpi. As compared to the rest of the cells, iMos expressed significantly higher levels of

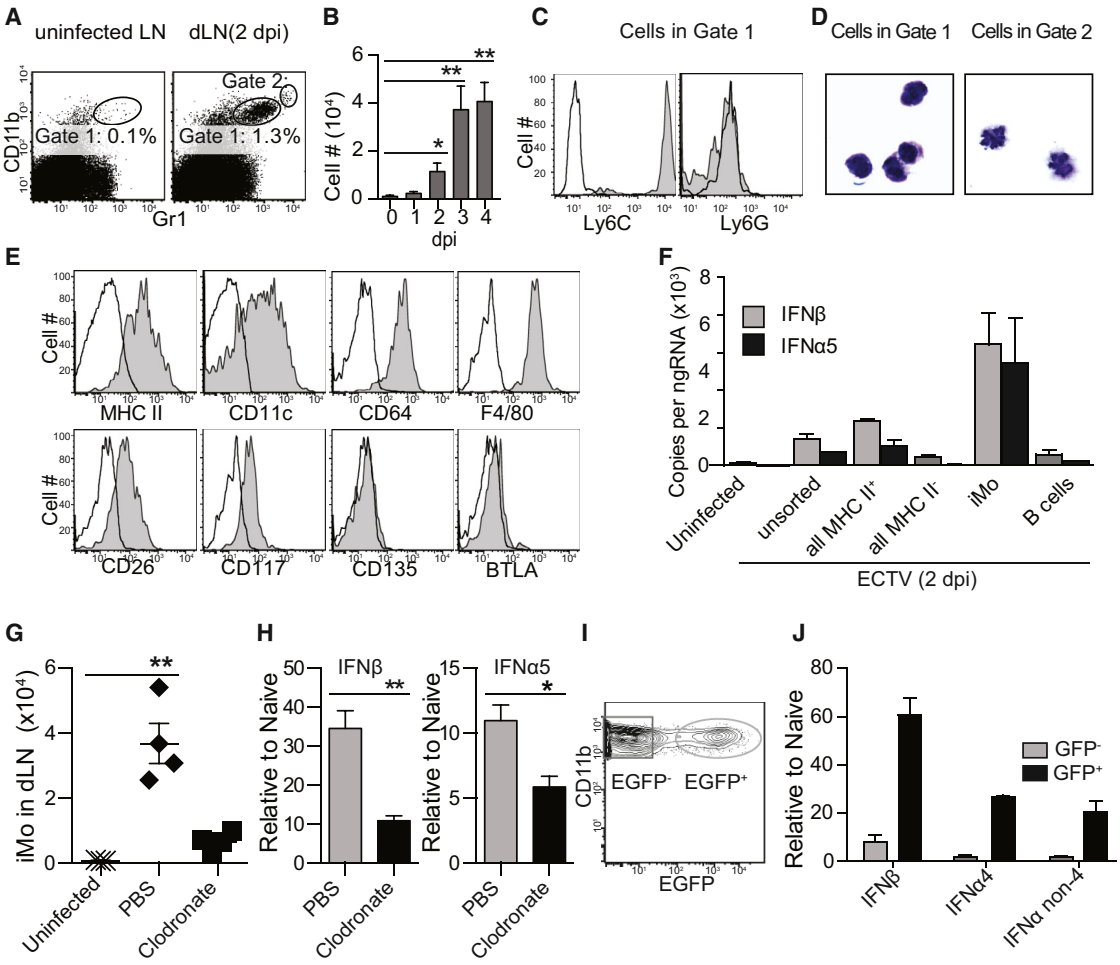

Figure 3. Infected Inflammatory Monocytes Are Responsible for Most of the IFN-I Expressed in the dLNs

(A) Representative flow cytometry plots depicting the gating and frequency of a population of $CD11b^{+}Gr1^{+}$ (gate 1) cells in the popliteal LNs of an uninfected mouse and in the dLNs of an infected mouse at 2.5 dpi with ECTV. A second gate (gate 2) with higher expression of the molecules (presumably neutrophils) is also shown.

(B) Number of cells in gate 1 at the indicated dpi. p values are compared to day 0. Data are displayed as the mean ± SEM of five mice per group in one experiment, which is representative of three similar experiments.

(C) At 2.5 dpi, gate 1 cells were analyzed for expression of the indicated molecules using specific mAbs (shaded) or isotype Ab as control (open). Data displayed as a representative sample of five mice per group. The experiment was repeated three times.

(D) At 2.5 dpi, gate 1 (left) and gate 2 (right) cells were sorted and stained with Giemsa. Data are representative of two experiments each with pools of five mice per group.

(E) As in (C). Gate 1 cells are now referred as inflammatory monocytes (iMos).

(F) IFN-I expression in unsorted cells or the indicated sorted cells from uninfected LNs or dLNs at 2.5 dpi. Data, displayed as mean ± SEM of pooled cells from five mice per group, are representative of two similar experiments. p values are not shown because the data correspond to two technical replicates.

(G) Number of iMos in the LNs of uninfected mice and at 2.5 dpi in the dLNs of mice treated intravenously with liposomes filled with PBS as a control or with clodronate to deplete monocytes and macrophages. Data, displayed as individual mice and mean ± SEM, correspond to an experiment with four mice per group, which is representative of two similar experiments.

(H) IFN-I expression at 2.5 dpi in the dLNs of mice receiving PBS or clodronate liposomes i.v. Data, shown as mean ± SEM, correspond to an experiment with five mice per group, which is representative of two similar experiments.

(I) Representative flow cytometry plot depicting EGFP and CD11b expression in the iMo gate from the dLNs at 2.5 dpi with ECTV-EGFP. $EGFP^{-}$ (uninfected) and $EGFP^{+}$ (infected).

(J) IFN-I expression in sorted $EGFP^{-}$ or $EGFP^{+}$ iMos gated as in (I). Data are displayed as mean ± SEM of pooled cells from five mice per group in one experiment, which is representative of two similar experiments. p values are not shown because the data correspond to two technical replicates.

For all, $^{*}p < 0.05$; $^{**}p < 0.01$.

several innate immune genes involved in IFN-I expression including *Tlr9*, *Myd88*, *M21d1* (which encodes *cGAS*), and *Irf7* but not *Tmem173*, *Irf3*, and *Nfkb1*. On the other side, B cells expressed significantly higher levels of only *Tlr9* and *Irf3* (Figure S2). As compared to controls, significantly fewer iMos were recruited to the dLNs of mice that had been inoculated intravenously with

liposomes filled with clodronate, known to deplete monocytes and macrophages in vivo (Figure 3G; Seiler et al., 1997; Van Rooijen, 1989). Moreover, mice treated with clodronate liposomes expressed significantly less IFN-I than those treated with PBS liposomes (Figure 3H).

Next, we infected mice with ECTV-EGFP and sorted infected ($EGFP^+$) and uninfected ($EGFP^-$) iMos from dLNs at 2.5 dpi (Figure 3I). We found that $EGFP^+$ iMos expressed significantly more IFN-I than $EGFP^-$ iMos (Figure 3J). Thus, infected iMos are the major producers of IFN-I in the dLNs of mice infected with ECTV.

The Recruitment of iMos Needs Extrinsic MyD88 whereas the Efficient Expression of IFN-I Requires Intrinsic STING

We next sought to identify the molecular mechanisms responsible for iMo recruitment. Compared to B6 mice, significantly fewer iMos were recruited into the dLNs of *Tlr9*$^{-/-}$ and *Myd88*$^{-/-}$ but not *Tmem173*^{gt} mice (Figure 4A). Hence, the recruitment of iMos into the dLNs requires TLR9-MyD88 but not STING. We next asked whether iMos require intrinsic and/or extrinsic MyD88 to accumulate in the dLNs and/or express IFN-I. For this, we used mixed bone marrow chimeras made with a 1:1 mixture of bone marrow from B6 congenic $CD45.1^+$ (WT) and $CD45.2^+$ *Myd88*$^{-/-}$ bone marrow transferred into WT mice (henceforth, WT+*Myd88*$^{-/-}$ chimeras; Figure 4B). At 2.5 dpi, WT and *Myd88*$^{-/-}$ iMos accumulated in the dLNs of WT+*Myd88*$^{-/-}$ chimeras at similar frequencies (Figures 4C and 4D). Of note, in WT+*Myd88*$^{-/-}$ chimeras infected with ECTV-EGFP, $EGFP^+$ *Myd88*$^{-/-}$ and $EGFP^+$ WT iMos expressed similar levels of IFN-I (Figure 4E). Conversely, in WT+*Tmem173*^{gt} chimeras, $EGFP^+$ *Tmem173*^{gt} iMos expressed significantly less IFN-I than $EGFP^+$ WT iMos (Figure 4F). Hence, to accumulate in the dLNs or produce IFN-I, iMos do not require intrinsic MyD88. However, they need intrinsic functional STING to efficiently express IFN-I.

The Accumulation of iMos in the dLNs Requires TLR9 and MyD88 Expression in Chemokine-Producing $CD11c^+$ Cells

Next, we crossed mice carrying *Cre* recombinase in different cell types with mice carrying floxed alleles of *Myd88* (*Myd88*$^{fl/fl}$) or *Tlr9* (*Tlr9*$^{fl/fl}$) to specifically eliminate MyD88 and TLR9 in cells of interest. Mice without Myd88 in hepatocytes (*Alb*-Cre *Myd88*$^{fl/fl}$, selected as controls because hepatocytes are late targets of ECTV infection) or in monocytes and macrophages (*Lyz2*-Cre *Myd88*$^{fl/fl}$) survived the infection. Conversely, most *Vav1*-Cre *Tlr9*$^{fl/fl}$ mice and all *Vav1*-Cre *Myd88*$^{fl/fl}$ mice, which are deficient in TLR9 and Myd88, respectively, in all hematopoietic cells, succumbed to mousepox. Similarly, most *Itgax*-Cre *Tlr9*$^{fl/fl}$ and all *Itgax*-Cre *Myd88*$^{fl/fl}$, which lack TLR9 and MyD88, respectively, in $CD11c^+$ cells, also died from mousepox (Figure 5A). Concordantly, iMos accumulated efficiently in the dLNs of *Alb*-Cre *Myd88*$^{fl/fl}$ and *Lyz2*-Cre *Myd88*$^{fl/fl}$ mice but poorly in the dLNs of *Vav1*-Cre *Myd88*$^{fl/fl}$, *Itgax*-Cre *Myd88*$^{fl/fl}$, *Vav1*-Cre *Tlr9*$^{fl/fl}$, and *Itgax*-Cre *Tlr9*$^{fl/fl}$ mice (Figures 5B and 5C). Moreover, *Vav1*-Cre *Myd88*$^{fl/fl}$ and *Itgax*-Cre *Myd88*$^{fl/fl}$ mice expressed significantly lower levels of IFN-I in the dLNs than *Alb*-Cre *Myd88*$^{fl/fl}$ mice, whereas normal levels were detected in *Lyz2*-Cre *Myd88*$^{fl/fl}$ mice (Figure 5D).

We next sought to understand why extrinsic TLR9 and MyD88 are required to recruit iMos to the dLNs. Because chemokine gradients regulate leukocyte migration (Griffith et al., 2014), we used RT-qPCR to determine which chemokines were upregulated in the dLNs at 1 dpi in a TLR9- and MyD88-dependent manner. We found that CCL2 and CCL7 (Figure 5E), which are ligands for the chemokine receptor CCR2 and known to be involved in the recruitment of iMos to inflamed tissues (Griffith et al., 2014), were upregulated in B6 but not in *Tlr9*$^{-/-}$, *Vav1*-Cre^+ *Myd88*$^{fl/fl}$, *Itgax*-Cre^+ *Myd88*$^{fl/fl}$, *Vav1*-Cre^+ *Tlr9*$^{fl/fl}$, and *Itgax*-Cre^+ *Tlr9*$^{fl/fl}$ mice. This suggested that CCL2 and CCL7, induced by TLR9 and MyD88 signaling, might be involved in the recruitment of iMos to the dLNs. In agreement, mice deficient in CCL7 (*Ccl7*$^{-/-}$) recruited significantly fewer iMos to the dLNs than B6 mice upon ECTV infection. The impaired recruitment of iMos in *Ccl7*$^{-/-}$ mice was exacerbated by treatment with the CCR2 antagonist RS102895 (Figure 5F; Giunti et al., 2006). These data suggest that the efficient recruitment of iMos to the dLNs requires expression of CCR2-binding chemokines and that this expression requires intrinsic TLR9 and MyD88 in $CD11c^+$ cells. Of note, iMos were still the key cells that expressed IFN-I in RS102895-treated *Ccl7*$^{-/-}$ mice (Figure S3A). Yet, despite the reduced number of iMos, we did not detect significant differences in the levels of IFN-I in the dLNs of B6 and RS102895-treated *Ccl7*$^{-/-}$ mice (not shown). Although we do not know the reason for the lack of significant differences, we have found that RS102895-treated *Ccl7*$^{-/-}$ mice have significantly higher virus loads than B6 mice in the dLNs at 2.5 dpi and iMos are still the major producers of IFN-I (Figure S3B). Perhaps this increase in virus loads somehow compensates for the decrease in iMos.

IRF7 Is Required for the Efficient Recruitment of iMos and IFN-I Expression in the dLNs

Next, we sought to identify the transcription factors downstream of TLR9-MyD88 and STING necessary for the accumulation of iMos in the dLNs and for their expression of IFN-I. It is well established that TLR9-MyD88 signaling activates the transcription factors IRF7 and NF-κB (Orzalli and Knipe, 2014), whereas STING mainly activates IRF3 and NF-κB (Wu and Chen, 2014) but can also activate IRF7 (Ishikawa and Barber, 2008). As we previously reported, B6 mice that lack the transcription factor IRF7 (*Irf7*$^{-/-}$) are susceptible to mousepox whereas B6 mice that lack IRF3 (*Irf3*$^{-/-}$) are resistant (Rubio et al., 2013). Similar to *Myd88*$^{-/-}$ mice, *Irf7*$^{-/-}$ mice were more susceptible to ECTV infection than STING-deficient mice because 100% of *Irf7*$^{-/-}$ and *Myd88*$^{-/-}$ but only 80% of *Tmem173*^{gt} mice succumbed to mousepox (not shown). Also, the livers of *Irf7*$^{-/-}$ mice showed severe pathology as determined by histology and immunohistochemistry (Figure 6A). Accordingly, the virus titers in the livers of *Irf7*$^{-/-}$ mice were as high as those in *Myd88*$^{-/-}$ mice (Figure 6B). Consistent with being downstream of MyD88, the virus titers in *Irf7*$^{-/-}$ mice were similar to those in *Myd88*$^{-/-}$ mice but significantly higher than in *Tmem173*^{gt} mice ($p < 0.01$). Also phenocopying MyD88 deficiency, the recruitment of iMos to the dLNs of *Irf7*$^{-/-}$ mice was impaired (Figure 6C). Furthermore, the expression of IFN-I in the dLNs of *Irf7*$^{-/-}$ mice was as low as in the dLNs of *Myd88*$^{-/-}$ mice and

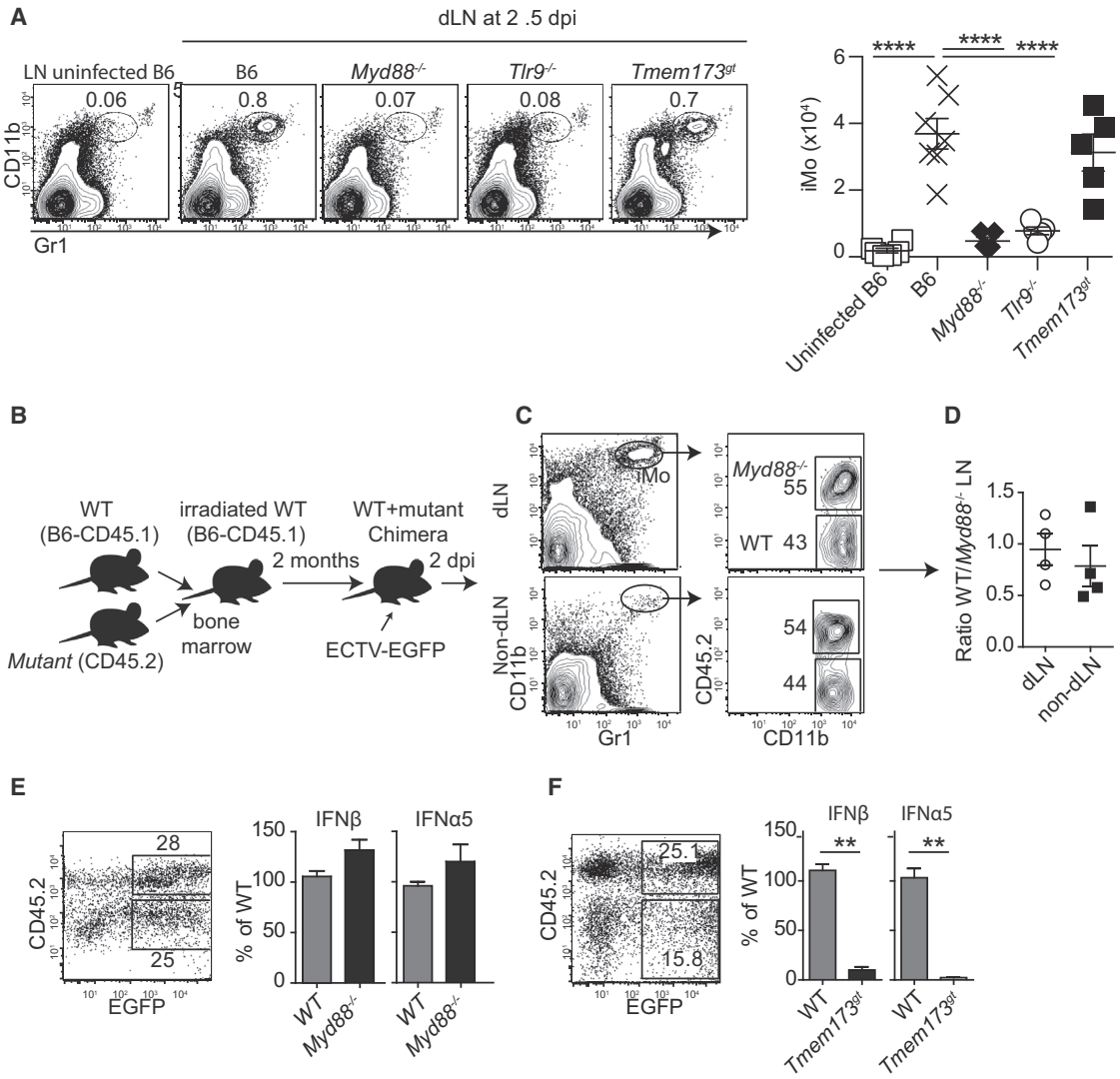

Figure 4. The Recruitment of iMos Needs Extrinsic MyD88 whereas the Efficient Expression of IFN-I Requires Intrinsic STING

(A) The indicated mice were infected with ECTV and at 2.5 dpi, their dLNs were analyzed for the presence of iMos. Representative flow cytometry plots (left) and the calculated numbers of iMos (right) are shown. Data, shown as individual mice and mean ± SEM, correspond to an experiment with five mice per group, which is representative of two similar experiments.

(B) Diagram of the experiments in (C)–(F).

(C) Representative flow cytometry plots of the dLNs and non-dLNs of WT+*Myd88*$^{-/-}$ chimeras at 2.5 dpi. The plots on the left show CD11b and Gr1 staining with the iMo gates marked. The plots on the right show the expression of CD45.2 and CD11c in the iMo gates. The gates for mutant (CD45.2^{+}) and WT (CD45.2^{-}) iMos are shown.

(D) Ratio of WT/*Myd88*$^{-/-}$ iMos in the dLNs of WT+*Myd88*$^{-/-}$ chimeras. Data, shown as individual mice and mean ± SEM, correspond to an experiment with four mice per group, which is representative of two similar experiments.

(E) Representative flow cytometry plot for EGFP and CD45.2 expression in gated iMos from dLNs of WT+*Myd88*$^{-/-}$ chimeras at 2.5 dpi with ECTV-EGFP (left) and IFN-I expression in the sorted EGFP^{+} WT and EGFP^{+} *Myd88*$^{-/-}$ iMos (right). Data are for pooled cells from five mice per group and representative of two similar experiments. Means ± SEM of three technical replicates are shown.

(F) As in (E) but with cells from WT+*Tmem173*^{gt} chimeras.

For all, *p < 0.05; **p < 0.01; ***p < 0.001; ****p < 0.0001.

significantly lower than in the dLNs of *Tmem173*^{gt} mice (Figure 6D). In addition, *Irf7*$^{-/-}$ mice did not upregulate the expression of *Ccl2* and *Ccl7* in the dLNs (Figure 6E). Together, these data suggest that the expression of the chemokines that recruit iMos to the dLNs requires the transcription factor IRF7 downstream of TLR9-MyD88.

Inflammatory Monocytes Require Intrinsic STING-IRF7 and STING-NF-κB to Express IFN-α and IFN-β, Respectively

We next determined whether iMos require intrinsic IRF7 to express IFN-α and IFN-β. We found that infected iMos obtained at 2.5 dpi with ECTV-EGFP from the dLNs of *Tmem173*^{gt} mice

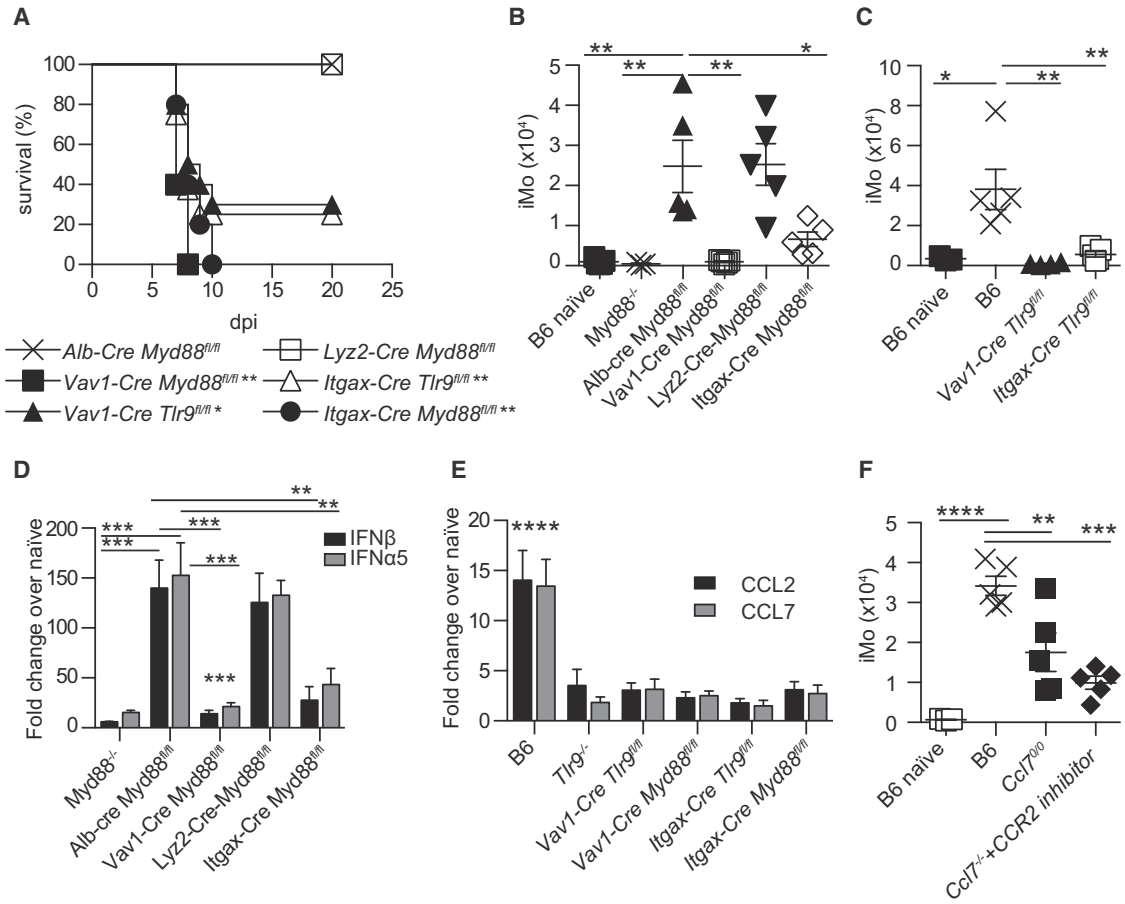

Figure 5. The Accumulation of iMos in the dLNs Requires TLR9 and MyD88 in Chemokine-Producing CD11c$^+$ Cells

(A) Survival of the indicated mice to ECTV infection. Data correspond to one experiment with five mice per group and is representative of three similar experiments. p values are compared to *Alb*-Cre *Myd88*$^{fl/fl}$ mice.

(B) Calculated number of iMos in the dLNs of the indicated mice at 2.5 dpi. Data, displayed as individual mice with mean ± SEM, correspond to one experiment with five mice per group, which is representative of three similar experiments.

(C) As in (B), but for indicated mice.

(D) Expression of IFN-I in the dLNs of the indicated mice at 2.5 dpi. p values are compared to *Alb*-Cre *Myd88*$^{fl/fl}$ mice. Data, displayed as mean ± SEM, correspond to one experiment with five mice per group, which is representative of three similar experiments.

(E) *Ccl2* and *Ccl7* expression in the dLNs at 1 dpi. p values are compared to naive B6 mice (not shown) and are similar for *Ccl2* and *Ccl7*. Data displayed as in (E).

(F) As in (B), but for indicated mice.

For all, *p < 0.05; **p < 0.01; ***p < 0.001; ****p < 0.0001.

expressed IFN-β inefficiently, whereas those from *Irf3*$^{-/-}$ and *Irf7*$^{-/-}$ mice expressed as much IFN-β as iMos from WT B6 mice. In contrast, infected iMos from the dLNs of *Irf3*$^{-/-}$ mice expressed as much "early" IFN-α4 and "late" IFN-α5 as those from WT mice, but those from *Tmem173*^{gt} and the few present in *Irf7*$^{-/-}$ mice expressed significantly less (Figure 7A). Therefore, the signaling pathways for IFN-α and IFN-β expression diverge downstream of STING, with IRF7 being required for efficient IFN-α but not IFN-β expression.

Given our previous finding of a crosstalk between the NF-κB and IFN-I pathways during ECTV infection (Rubio et al., 2013), we speculated that in ECTV-infected iMos, NF-κB is the transcription factor downstream of STING that is responsible for the expression of IFN-β. However, we were unable to directly test this idea in *Nfkb1*$^{-/-}$ mice, because these mice lack popliteal lymph nodes (Rubio et al., 2013). Thus, we produced WT+*Nfkb1*$^{-/-}$ and also WT+*Irf7*$^{-/-}$ bone marrow chimeras (Figures 7B–7E). In both types of chimeras, WT and mutant iMos accumulated in the dLNs at similar frequencies (not shown). Hence, iMos do not need intrinsic NF-κB or IRF7 to accumulate in the dLNs. When tested for IFN-I expression, *Irf7*$^{-/-}$ iMos expressed significantly less early IFN-α4 and late IFN-α5 than WT iMos but the levels of early IFN-β were similar. On the other hand, *Nfkb1*$^{-/-}$ iMos expressed as much early and late IFN-α but significantly less IFN-β than WT iMos. Thus, in ECTV-infected iMos, efficient transcription of early and late IFN-α requires IRF7 whereas the expression of IFN-β is mostly dependent on NF-κB transcription.

DISCUSSION

We have studied how different pathways of pathogen sensing and cell types contribute to IFN-I expression and resistance to

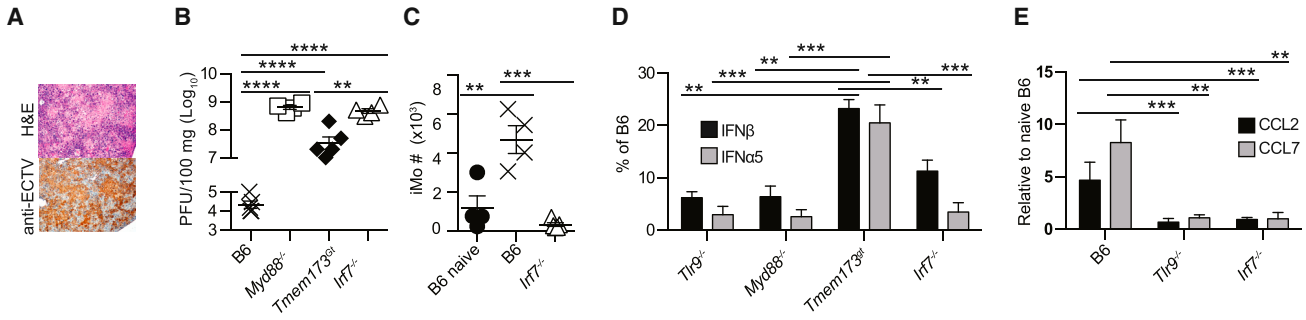

Figure 6. IRF7 Is Required for the Efficient Recruitment of iMos and IFN-I Expression in the dLNs

(A) Representative liver sections from *Irf7*$^{-/-}$ mice at 7 dpi stained with H&E (top) or with anti-ECTV Ab (bottom). The experiment was performed three times with four or five mice per group with similar results.

(B) ECTV titers in the liver of the indicated mice at 7 dpi. Data, displayed as individual mice with mean ± SEM, correspond to one experiment with four or five mice per group, which is representative of three similar experiments.

(C) Numbers of iMos in the dLNs of the indicated mice at 2.5 dpi. Data as in (B).

(D) IFN-I in the dLNs of the indicated mice at 2.5 dpi expressed as percent of the values for the same interferon in infected B6 mice. Data, displayed as mean ± SEM, correspond to one experiment with five mice per group, which is representative of three similar experiments.

(E) Expression of the indicated chemokines in the dLNs of the indicated mice at 1 dpi. Data as in (D).

For all, *p < 0.05; **p < 0.01; ***p < 0.001; ****p < 0.0001.

a highly lethal infection caused by ECTV, a DNA virus of the genus Orthopoxvirus that also includes variola virus (VARV, the virus that causes smallpox) and vaccinia virus (VACV, the smallpox vaccine). For this purpose, we have focused on the dLNs because of its critical role in restricting viral spread (Fang et al., 2008; Junt et al., 2007; Kastenmüller et al., 2012).

The most important aspect of our work is the finding that the DNA-sensing pathways TLR9-MyD88-IRF7 and STING-IRF7-NF-κB are essential for efficient IFN-I production and resistance to mousepox but that their respective roles in IFN-I expression are very different: the TLR9-MyD88-IRF7 pathway is required in CD11c^{+} cells for the expression in the dLNs of CCR2 ligands—and probably other pro-inflammatory molecules necessary for the efficient recruitment of iMos to the dLNs—whereas the STING-IRF7 and STING-NF-κB axes are needed for IFN-I expression in infected iMos. That STING is necessary for IFN-I expression is consistent with the recent finding that STING is required for IFN-I expression in mouse cDCs infected with modified VACV strain Ankara (MVA) (Dai et al., 2014). Although we have ruled out DAI as the critical DNA sensor, we have not yet identified which is the receptor upstream of STING that senses ECTV to drive IFN-I expression. We hypothesize the key sensor is cGAS, because cGAS-STING is used by mouse cDCs (Dai et al., 2014; Li et al., 2013), mouse macrophages and fibroblasts (Li et al., 2013), and human embryonic kidney 293 cells (Ablasser et al., 2013) to produce IFN-I in vitro after infection with WT VACV or MVA.

We have also ruled out TRIF and MAVS as key players in IFN-I expression and resistance to mousepox after ECTV infection. That TRIF is not essential is not surprising because TLR9 uses MyD88 but not TRIF as the adaptor, and because TLR9 is the only TLR required for resistance to mousepox (Rubio et al., 2013; Samuelsson et al., 2008; Sutherland et al., 2011). However, the finding that MAVS has no role is unexpected, because MAVS transduces signals from RNA-sensing RLRs, and it has been shown that in cultured cells, VACV, which is very similar to ECTV, produces RNA species that can activate these pathways and induce IFN-I expression (Myskiw et al., 2011; Pichlmair et al., 2009).

We also found that pDCs are not required for IFN-I expression or survival to ECTV infection. pDCs, which express RNA- and DNA-sensing TLR7, TLR8, and TLR9, have been touted as professional IFN-I producers (Gilliet et al., 2008). However, they have been proven not essential for IFN-I expression and/or resistance to infection in various infectious mouse models including vesicular stomatitis virus, influenza virus, mouse cytomegalovirus, and lymphocytic choriomeningitis virus (Reizis et al., 2011). Furthermore, it has been shown that pDCs contribute to IFN-I expression to systemic but not local infection with HSV-1, another large DNA virus (Swiecki et al., 2013). That pDCs are not essential for resistance to ECTV is in contrast to the findings of Tahiliani et al. (2013), who recently reported that mice depleted of pDCs succumbed to mousepox. Although that study did not examine IFN-I expression after infection, we attribute this discrepancy to differences in anti-BST2 mAb clones and doses between our study and theirs and the possible depletion of other cell types by this type of mAbs (Swiecki and Colonna, 2010).

The finding that the cells that exclusively express IFN-I in the dLNs are infected iMos is novel and unexpected because these cells are not considered professional IFN-I producers. Nevertheless, it has been shown that Ly6C^{+} iMos use TLR2 to produce IFN-I during VACV infection (Barbalat et al., 2009) and that iMos produce IFN-β in response to *Toxoplasma gondii* (Han et al., 2014). Moreover, other myeloid cells have been found to produce IFN-I. For example, conventional DCs (cDCs) produce IFN-I in response to lymphocytic choriomeningitis virus (Diebold et al., 2003), reovirus (Johansson et al., 2007), and rotavirus (Lopez-Guerrero et al., 2010) in vivo. Also, cDCs and macrophages express IFN-I in response to herpes simplex virus (Rasmussen et al., 2007) and alveolar macrophages in response to Newcastle disease virus (Kumagai et al., 2007). In culture,

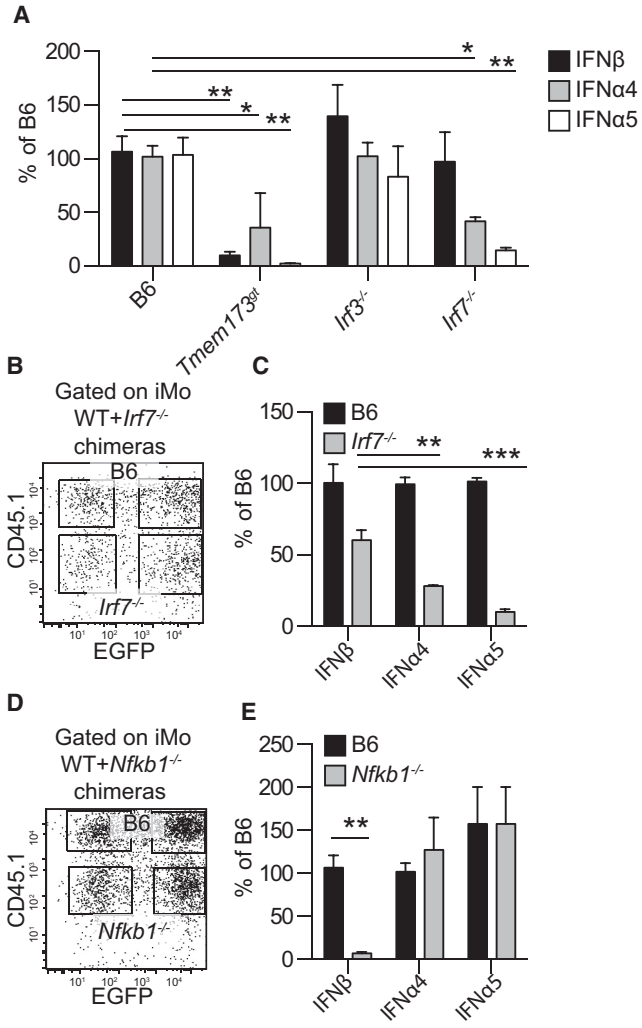

Figure 7. Inflammatory Monocytes Require Intrinsic STING-IRF7 and STING-NF-κB to Express IFN-α and IFN-β, Respectively

(A) Expression of IFN-I in sorted EGFP$^+$ iMos sorted from the dLNs of the indicated mice at 2.5 dpi. Data, displayed as mean ± SEM from one experiment representative of three, correspond to pooled cells from five mice per group and three technical replicates.

(B) Representative flow cytometry plots of gated iMos from the dLNs at 2.5 dpi of WT+ *Irf7*$^{-/-}$ chimeras showing CD45.1 and EGFP expression (left).

(C) IFN-I expression in sorted infected (EGFP$^+$) WT (CD45.1$^+$) and *Irf7*$^{-/-}$ (CD45.1$^-$) iMos from WT+*Irf7*$^{-/-}$ chimeras as identified in (B). Data, displayed as mean ± SEM from one experiment representative of three, correspond to pooled cells from five mice per group and three technical replicates.

(D) As in (B) but for WT+*Nfkb1*$^{-/-}$ chimeras.

(E) As in (C) but for WT+*Nfkb1*$^{-/-}$ chimeras.

For all, *p < 0.05; **p < 0.01; ***p < 0.001.

influenza-virus-infected human monocyte-derived DCs also produce IFN-I (Cao et al., 2012).

The discoveries that iMos express IFN-I only if they are infected and that STING is the critical adaptor are internally consistent. STING is used by PRRs that recognize the presence of PAMPs in the cytosol, which indicates an ongoing infection. Interestingly, although B cells constitute the vast majority of infected cells in the dLNs, they failed to express IFN-I. A possible reason is that when compared to monocytes, they express low levels of IRF7 and the cytosolic DNA sensors IFI16 (*Ifi204*) and cGAS (*E330016A19Rik*) as indicated in the Immgen database (http://www.immgen.org) and as suggested by our own RT-qPCR analysis.

The identity and residence of the CD11c$^+$ cells in which the TLR9-MyD88-IRF7 pathway is needed for CCR2-ligand expression still needs to be elucidated. One possibility is that they are Langerhans cells or dermal DCs that reside in the footpad and migrate to the dLNs in a TLR9-MyD88-dependent manner (Martín-Fontecha et al., 2009). It is also possible that these cells are DCs that reside in the subcapsular space that have recently shown to be the first to capture particulate antigens in the dLNs (Radtke et al., 2015). We speculate that CD11c$^+$ cells need TLR9-MyD88 intrinsically to express the CCR2 ligands and probably other inflammatory cytokines that are required for iMo migration. However, it remains possible that the role of TLR9-MyD88 in CD11c$^+$ cells is also indirect for this function. Regardless of this, iMos migrate to the dLNs in response to signals that depend on TLR9-MyD88 in CD11c$^+$ cells. After migrating to the dLNs, iMos become targets of infection and, consequently, the major producers of IFN-I in the dLNs. Notably, iMos do not need intrinsic MyD88 to migrate to the dLNs or to produce IFN-I; instead, they rely on intrinsic STING-IRF7 and STING-NF-κB signaling for expression of IFN-α and IFN-β, respectively.

The most frequently studied IRF downstream of STING is IRF3 (Wu and Chen, 2014). Therefore, it might be surprising that the expression of IFN-I is not altered in *Irf3*$^{-/-}$ mice. However, it has been shown that STING can directly activate IRF7 (Ishikawa and Barber, 2008). Moreover, IRF7 is expressed at much higher levels than IRF3 in most myeloid cells (http://www.immgen.org), and in our own experiments, IRF7 but not IRF3 was expressed at higher levels in iMos than in other cells. This suggests that in iMos, STING-IRF7 signaling makes IRF3 redundant.

Our experiments suggest that iMos have additional pathways for IFN-I expression because infected iMos deficient in *Irf7*$^{-/-}$ and *Tmem173*^{gt} expressed detectable (albeit significantly reduced) IFN-I. Although insufficient to protect most mice from lethal mousepox, these alternate pathways might explain why *Tmem173*^{gt} mice, which recruit iMos to the dLNs, are less susceptible than MyD88 and IRF7 mice, which do not recruit iMos to the dLNs.

We also found that the expression of IFN-β in iMos is strictly dependent on NF-κB, even though the *ifnb1* enhancer has binding sites for NF-κB, IRF3, and IRF7 (Honda et al., 2005). Merika et al. (1998) have shown that NF-κB p65 is needed for the initial capture and stabilization of CBP-p300 at the enhanceosome, so probably this role for NF-κB is more critical in driving IFN-β expression in iMos than it is in MEFs, where NF-κB appears largely dispensable for virus-driven IFN-β expression (Balachandran and Beg, 2011; Wang et al., 2007).

In summary, we have identified iMos as the cell type critical for IFN-I production in the dLNs after infection with a poxvirus through its biological route in its natural host. Moreover, we show that two DNA-sensing pathways, both traditionally associated with a direct role in IFN-I expression, play distinct but sequentially roles in different cell types: the TLR9-MyD88-IRF7 pathway functions in CD11c$^+$ cells to recruit iMos to the dLNs and the STING-IRF7 and STING-NF-κB pathways are directly

responsible for IFN-I production after iMo infection. Together, these results provide important insights into how distinct pathogen-sensing mechanisms co-operate to recognize and limit pathogen spread in vivo.

EXPERIMENTAL PROCEDURES

Mice and Animal Experiments

All the procedures involving mice were carried out in strict accordance with the recommendations in the Guide for the Care and Use of Laboratory Animals of the NIH. All protocols were approved by Fox Chase Cancer Center's (FCCC) Institutional Animal Care and Use Committee. B6 (C57BL/6, CD45.2$^+$; Taconic) and B6-LY5.1/Cr (B6-CD45.1, CD45.1$^+$; NCI-Charles River) mice were purchased at 6–8 weeks of age. All other mice, in a B6 background, were bred at FCCC from original breeders obtained from different sources and used at an age of 6–16 weeks. *Vav1*-Cre (B6.Cg-Tg(*Vav1-cre*)^{A2Kio}/J), *Alb*-Cre (B6.Cg-Tg(*Alb-cre*)^{21Man}/J), *Lyz2*-Cre (B6.129P2-*Lyz2*$^{tm1(cre)Ifo}$/J), *Itgax*-Cre (B6.Cg-Tg(*Itgax-cre*)$^{1-1Reiz}$/J), *Ccl7*$^{-/-}$ (B6.129S4-*Ccl7*^{tm1ifc}/J), *Nfkb1*$^{-/-}$ (B6.Cg-*Nfkb1*^{tm1Bal}/J), *Myd88*$^{fl/fl}$ (B6.129P2(SJL)-Myd88^{tm1Defr}/J), *Tmem173*^{gt} (C57BL/6J-*Tmem173*^{gt}/J), *Tlr2*$^{-/-}$ (B6.129-*Tlr2*^{tm1Kir}/J), and *Il1r*$^{-/-}$ (B6.129S7-*Il1r1*^{tm1Imx}/J) mice were originally purchased from Jackson Laboratories. B6.129-*Tlr9*^{tm1}Aki/Obs (*Tlr9*$^{-/-}$) and B6.129-*Myd88*^{tm1}Aki/Obs (*Myd88*$^{-/-}$) mice were produced by Dr. S. Akira (Osaka University, Japan) (Adachi et al., 1998; Hemmi et al., 2000) and generously provided by Dr. Robert Finberg (University of Massachusetts, Worcester, MA). *Irf7*$^{-/-}$ (B6.129P2-Irf7^{tm1Ttg}/TtgRbrc), *Irf3*$^{-/-}$ (B6;129S6-Irf3^{tm1Ttg}/TtgRbrc), and B6.129B6-*Mavs*^{tm1Tsse} were from Riken Bioresource Center (Tsukuba, Japan). *Ifnar1*$^{-/-}$ mice backcrossed to B6 (Moltedo et al., 2011) were a gift from Dr. Thomas Moran (Mount Sinai School of Medicine, New York, NY), and *Zbp1*$^{-/-}$ mice (Ishii et al., 2008) were a gift from Dr. S. Akira. *Tlr9*$^{fl/fl}$ mice were produced in the M.S. laboratory and will be described in detail elsewhere. In brief, LoxP sites were inserted flanking exon 2, which contains virtually all of the protein coding sequences, of TLR9. The mutant allele was created in B6x129 ES cells (line BA1) and proper targeting was confirmed by PCR, Southern blotting, and sequencing. Subsequent to germline transmission, the floxed NeoR gene that was part of the original construct was deleted by breeding to a mouse line that expressed Cre-recombinase and the proper deletion again confirmed by Southern blot. The resulting mice were bred to B6 mice for ten generations before crossing with the Cre-deleter mice obtained from Jackson.

Production of Bone Marrow Chimeric Mice

Bone marrow chimeras were prepared as previously described (Sigal et al., 1999; Xu et al., 2010) using 5- to 7-week-old mice as donors and recipients. For mixed bone marrow chimeras, bone marrow cells from the two donor types were mixed at 1:1 ratio. Chimeras were used in experiments 6–8 weeks after reconstitution.

Viruses and Infection

Virus stocks, including ECTV Moscow strain (ATCC VR-1374) and ECTV-EGFP (Fang et al., 2008), were propagated in tissue culture as previously described (Xu et al., 2008). Mice were infected in the footpad with 3,000 plaque forming units (PFUs) ECTV WT or ECTV-*EGFP* as indicated. For the determination of survival, the mice were monitored daily. To avoid unnecessary suffering, mice were euthanized and counted as dead when imminent death was certain as determined by lack of activity and unresponsiveness to touch. For virus titers, the entire spleen or portions of the liver were homogenized in PBS using a Tissue Lyser (QIAGEN). Virus titers were determined on BS-C-1 cells as before (Xu et al., 2008).

Cell Depletions

To deplete pDCs, B6 mice were injected with 500 μg rat mAb 927 or control rat IgG (Blasius et al., 2006) 1 day before and 1 day after infection with ECTV. Efficient depletion of pDCs was confirmed by flow cytometry using mAbs B220 and 400c (anti-Siglec-H) on inguinal LNs and spleen at 2 days after the second depletion. To deplete monocytes/macrophages, mice received 200 μl clodronate-liposomes diluted to 5 mg/ml clodronate or control PBS-liposomes intravenously 2 days before infection.

Flow Cytometry

Flow cytometry was performed as previously described (Xu et al., 2008). mAbs to CD3 (145-2C11), CD4 (GK1.5), CD8a (53–6.7), CD11c (N418), IFN-γ (XMG1.2), CD64 (X54-5/7.1), F4/80 (BM8), CD135 (Flt3, clone A2F10), CD117 (c-Kit, clone 2B8), CD272 (6A6), CD26 (H194-112), IA/IE (M5/114.15.2), Ly-6G (IA8), Ly-6C (HK1.4), B220 (RA3-6B2), CD317 (BST2, PDCA-1, Clone 927), and CXCL9 (MIG-2F5.5) were from Biolegend. mAbs to CD45.1 (A20), CD45.2 (104), Ly-6G and Ly-6C (Gr-1, Clone RB6-8C5), B220 (RA3-6B2), and CD11b (H194-112) were from BD Biosciences. mAb to Siglec-H (eBio440c) was from eBioscience.

To obtain single-cell suspensions, LNs were minced and dissociated in Liberase TM (1.67 Wünsch units/ml) and DNase I (0.2 mg/ml; Roche Diagnostics) in PBS with 25 mM of HEPES for 30 min at 37°C. Liberase digestion was followed by mechanical disruption of the tissue through a 70-μm filter. Cells were washed once with complete RPMI medium before surface staining. For analysis, samples were acquired using a BD LSR II flow cytometer (BD Biosciences), and data were analyzed with FlowJo software (TreeStar). For cell sorting, samples were acquired with a BD FACSAria III sorter (BD Biosciences).

Histopathology

Livers were harvested and fixed with formalin and stained with H&E or with rabbit anti-EVM135 as previously described (Xu et al., 2012). Sorted cells were stained using a standard Wright-Giemsa protocol.

RNA Preparation and RT-qPCR

Total RNA from LNs was obtained with the RNeasy Mini Kit (QIAGEN) as previously described (Rubio et al., 2013; Xu et al., 2012). Total RNA from sorted cells (10^4–10^5 cells) was extracted with Trizol reagent (Life Technologies) according to the manufacturer's instructions. In brief, ~10^4 cells were added into 1 ml of Trizol. When precipitating RNA, 10 μg of RNase-free glycogen (Invitrogen) was added to the aqueous phase as a carrier. First-strand cDNA was synthesized with High Capacity cDNA Reverse Transcription Kit (Lift Technologies). qPCR was performed as before (Rubio et al., 2013; Xu et al., 2012) using probes from the Universal Library (Roche) and the oligonucleotides suggested by the manufacturer's software.

Statistics

Data were analyzed with Prism 6 software (GraphPad Software). For survival we used the Log-rank (Mantel-Cox). For other experiments, ANOVA with Tukey correction for multiple comparisons or Student's t test were used as applicable. In all figures, *p < 0.05; **p < 0.01; ***p < 0.001; ****p < 0.0001.

SUPPLEMENTAL INFORMATION

Supplemental Information includes three figures and can be found with this article online at http://dx.doi.org/10.1016/j.immuni.2015.11.015.

ACKNOWLEDGMENTS

We thank Ms. Holly Gillin for assistance in the preparation of the manuscript and Dr. Siddharth Balachandran for critical reading. We also thank the Fox Chase Cancer Center (FCCC) Laboratory Animal, Flow Cytometry, and Tissue Culture Facilities for their services. This work was supported by NIH grants R01AI065544, R01AI110457, and U19AI083008 to L.J.S. and P30CA006927 to the FCCC. S.R. was supported by T32 CA-009035036 to FCCC. A generous gift form the Kirby Foundation also contributed to funding this work.

Received: April 8, 2015
Revised: June 29, 2015
Accepted: November 19, 2015
Published: December 15, 2015

REFERENCES

Ablasser, A., Schmid-Burgk, J.L., Hemmerling, I., Horvath, G.L., Schmidt, T., Latz, E., and Hornung, V. (2013). Cell intrinsic immunity spreads to bystander cells via the intercellular transfer of cGAMP. Nature *503*, 530–534.

Adachi, O., Kawai, T., Takeda, K., Matsumoto, M., Tsutsui, H., Sakagami, M., Nakanishi, K., and Akira, S. (1998). Targeted disruption of the MyD88 gene results in loss of IL-1- and IL-18-mediated function. Immunity *9*, 143–150.

Ahmad-Nejad, P., Häcker, H., Rutz, M., Bauer, S., Vabulas, R.M., and Wagner, H. (2002). Bacterial CpG-DNA and lipopolysaccharides activate Toll-like receptors at distinct cellular compartments. Eur. J. Immunol. *32*, 1958–1968.

Balachandran, S., and Beg, A.A. (2011). Defining emerging roles for NF-κB in antivirus responses: revisiting the interferon-β enhanceosome paradigm. PLoS Pathog. *7*, e1002165.

Barbalat, R., Lau, L., Locksley, R.M., and Barton, G.M. (2009). Toll-like receptor 2 on inflammatory monocytes induces type I interferon in response to viral but not bacterial ligands. Nat. Immunol. *10*, 1200–1207.

Blasius, A.L., Giurisato, E., Cella, M., Schreiber, R.D., Shaw, A.S., and Colonna, M. (2006). Bone marrow stromal cell antigen 2 is a specific marker of type I IFN-producing cells in the naive mouse, but a promiscuous cell surface antigen following IFN stimulation. J. Immunol. *177*, 3260–3265.

Cao, W., Taylor, A.K., Biber, R.E., Davis, W.G., Kim, J.H., Reber, A.J., Chirkova, T., De La Cruz, J.A., Pandey, A., Ranjan, P., et al. (2012). Rapid differentiation of monocytes into type I IFN-producing myeloid dendritic cells as an antiviral strategy against influenza virus infection. J. Immunol. *189*, 2257–2265.

Colonna, M., Trinchieri, G., and Liu, Y.J. (2004). Plasmacytoid dendritic cells in immunity. Nat. Immunol. *5*, 1219–1226.

Dai, P., Wang, W., Cao, H., Avogadri, F., Dai, L., Drexler, I., Joyce, J.A., Li, X.D., Chen, Z., Merghoub, T., et al. (2014). Modified vaccinia virus Ankara triggers type I IFN production in murine conventional dendritic cells via a cGAS/STING-mediated cytosolic DNA-sensing pathway. PLoS Pathog. *10*, e1003989.

Diebold, S.S., Montoya, M., Unger, H., Alexopoulou, L., Roy, P., Haswell, L.E., Al-Shamkhani, A., Flavell, R., Borrow, P., and Reis e Sousa, C. (2003). Viral infection switches non-plasmacytoid dendritic cells into high interferon producers. Nature *424*, 324–328.

Esteban, D.J., and Buller, R.M. (2005). Ectromelia virus: the causative agent of mousepox. J. Gen. Virol. *86*, 2645–2659.

Fang, M., Lanier, L.L., and Sigal, L.J. (2008). A role for NKG2D in NK cell-mediated resistance to poxvirus disease. PLoS Pathog. *4*, e30.

Fenner, F. (1948). The pathogenesis of the acute exanthems; an interpretation based on experimental investigations with mousepox; infectious ectromelia of mice. Lancet *2*, 915–920.

Flint, S.J., Enquist, L.W., Racanniello, V.R., and Skalka, A.M. (2009). Principles of Virology, Third Edition (Washington, DC: ASM Press).

Gautier, E.L., Shay, T., Miller, J., Greter, M., Jakubzick, C., Ivanov, S., Helft, J., Chow, A., Elpek, K.G., Gordonov, S., et al.; Immunological Genome Consortium (2012). Gene-expression profiles and transcriptional regulatory pathways that underlie the identity and diversity of mouse tissue macrophages. Nat. Immunol. *13*, 1118–1128.

Gilliet, M., Cao, W., and Liu, Y.J. (2008). Plasmacytoid dendritic cells: sensing nucleic acids in viral infection and autoimmune diseases. Nat. Rev. Immunol. *8*, 594–606.

Giunti, S., Pinach, S., Arnaldi, L., Viberti, G., Perin, P.C., Camussi, G., and Gruden, G. (2006). The MCP-1/CCR2 system has direct proinflammatory effects in human mesangial cells. Kidney Int. *69*, 856–863.

Goubau, D., Deddouche, S., and Reis e Sousa, C. (2013). Cytosolic sensing of viruses. Immunity *38*, 855–869.

Griffith, J.W., Sokol, C.L., and Luster, A.D. (2014). Chemokines and chemokine receptors: positioning cells for host defense and immunity. Annu. Rev. Immunol. *32*, 659–702.

Han, S.J., Melichar, H.J., Coombes, J.L., Chan, S.W., Koshy, A.A., Boothroyd, J.C., Barton, G.M., and Robey, E.A. (2014). Internalization and TLR-dependent type I interferon production by monocytes in response to *Toxoplasma gondii*. Immunol. Cell Biol. *92*, 872–881.

Hemmi, H., Takeuchi, O., Kawai, T., Kaisho, T., Sato, S., Sanjo, H., Matsumoto, M., Hoshino, K., Wagner, H., Takeda, K., and Akira, S. (2000). A Toll-like receptor recognizes bacterial DNA. Nature *408*, 740–745.

Honda, K., Yanai, H., Takaoka, A., and Taniguchi, T. (2005). Regulation of the type I IFN induction: a current view. Int. Immunol. *17*, 1367–1378.

Ishii, K.J., Kawagoe, T., Koyama, S., Matsui, K., Kumar, H., Kawai, T., Uematsu, S., Takeuchi, O., Takeshita, F., Coban, C., and Akira, S. (2008). TANK-binding kinase-1 delineates innate and adaptive immune responses to DNA vaccines. Nature *451*, 725–729.

Ishikawa, H., and Barber, G.N. (2008). STING is an endoplasmic reticulum adaptor that facilitates innate immune signalling. Nature *455*, 674–678.

Ito, T., Wang, Y.H., and Liu, Y.J. (2005). Plasmacytoid dendritic cell precursors/type I interferon-producing cells sense viral infection by Toll-like receptor (TLR) 7 and TLR9. Springer Semin. Immunopathol. *26*, 221–229.

Iwasaki, A., and Medzhitov, R. (2010). Regulation of adaptive immunity by the innate immune system. Science *327*, 291–295.

Johansson, C., Wetzel, J.D., He, J., Mikacenic, C., Dermody, T.S., and Kelsall, B.L. (2007). Type I interferons produced by hematopoietic cells protect mice against lethal infection by mammalian reovirus. J. Exp. Med. *204*, 1349–1358.

Junt, T., Moseman, E.A., Iannacone, M., Massberg, S., Lang, P.A., Boes, M., Fink, K., Henrickson, S.E., Shayakhmetov, D.M., Di Paolo, N.C., et al. (2007). Subcapsular sinus macrophages in lymph nodes clear lymph-borne viruses and present them to antiviral B cells. Nature *450*, 110–114.

Kastenmüller, W., Torabi-Parizi, P., Subramanian, N., Lämmermann, T., and Germain, R.N. (2012). A spatially-organized multicellular innate immune response in lymph nodes limits systemic pathogen spread. Cell *150*, 1235–1248.

Kumagai, Y., Takeuchi, O., Kato, H., Kumar, H., Matsui, K., Morii, E., Aozasa, K., Kawai, T., and Akira, S. (2007). Alveolar macrophages are the primary interferon-alpha producer in pulmonary infection with RNA viruses. Immunity *27*, 240–252.

Li, X.D., Wu, J., Gao, D., Wang, H., Sun, L., and Chen, Z.J. (2013). Pivotal roles of cGAS-cGAMP signaling in antiviral defense and immune adjuvant effects. Science *341*, 1390–1394.

Lopez-Guerrero, D.V., Meza-Perez, S., Ramirez-Pliego, O., Santana-Calderon, M.A., Espino-Solis, P., Gutierrez-Xicotencatl, L., Flores-Romo, L., and Esquivel-Guadarrama, F.R. (2010). Rotavirus infection activates dendritic cells from Peyer's patches in adult mice. J. Virol. *84*, 1856–1866.

Martín-Fontecha, A., Lanzavecchia, A., and Sallusto, F. (2009). Dendritic cell migration to peripheral lymph nodes. Handbook Exp. Pharmacol. *188*, 31–49.

Merika, M., Williams, A.J., Chen, G., Collins, T., and Thanos, D. (1998). Recruitment of CBP/p300 by the IFN beta enhanceosome is required for synergistic activation of transcription. Mol. Cell *1*, 277–287.

Miller, J.C., Brown, B.D., Shay, T., Gautier, E.L., Jojic, V., Cohain, A., Pandey, G., Leboeuf, M., Elpek, K.G., Helft, J., et al.; Immunological Genome Consortium (2012). Deciphering the transcriptional network of the dendritic cell lineage. Nat. Immunol. *13*, 888–899.

Moltedo, B., Li, W., Yount, J.S., and Moran, T.M. (2011). Unique type I interferon responses determine the functional fate of migratory lung dendritic cells during influenza virus infection. PLoS Pathog. *7*, e1002345.

Muzio, M., Ni, J., Feng, P., and Dixit, V.M. (1997). IRAK (Pelle) family member IRAK-2 and MyD88 as proximal mediators of IL-1 signaling. Science *278*, 1612–1615.

Myskiw, C., Arsenio, J., Booy, E.P., Hammett, C., Deschambault, Y., Gibson, S.B., and Cao, J. (2011). RNA species generated in vaccinia virus infected cells activate cell type-specific MDA5 or RIG-I dependent interferon gene transcription and PKR dependent apoptosis. Virology *413*, 183–193.

Orzalli, M.H., and Knipe, D.M. (2014). Cellular sensing of viral DNA and viral evasion mechanisms. Annu. Rev. Microbiol. *68*, 477–492.

Pichlmair, A., Schulz, O., Tan, C.P., Rehwinkel, J., Kato, H., Takeuchi, O., Akira, S., Way, M., Schiavo, G., and Reis e Sousa, C. (2009). Activation of MDA5 requires higher-order RNA structures generated during virus infection. J. Virol. *83*, 10761–10769.

Radtke, A.J., Kastenmüller, W., Espinosa, D.A., Gerner, M.Y., Tse, S.W., Sinnis, P., Germain, R.N., Zavala, F.P., and Cockburn, I.A. (2015). Lymph-node resident CD8α+ dendritic cells capture antigens from migratory malaria sporozoites and induce CD8+ T cell responses. PLoS Pathog. *11*, e1004637.

Rasmussen, S.B., Sørensen, L.N., Malmgaard, L., Ank, N., Baines, J.D., Chen, Z.J., and Paludan, S.R. (2007). Type I interferon production during herpes simplex virus infection is controlled by cell-type-specific viral recognition through Toll-like receptor 9, the mitochondrial antiviral signaling protein pathway, and novel recognition systems. J. Virol. *81*, 13315–13324.

Reizis, B., Bunin, A., Ghosh, H.S., Lewis, K.L., and Sisirak, V. (2011). Plasmacytoid dendritic cells: recent progress and open questions. Annu. Rev. Immunol. *29*, 163–183.

Rubio, D., Xu, R.H., Remakus, S., Krouse, T.E., Truckenmiller, M.E., Thapa, R.J., Balachandran, S., Alcamí, A., Norbury, C.C., and Sigal, L.J. (2013). Crosstalk between the type 1 interferon and nuclear factor kappa B pathways confers resistance to a lethal virus infection. Cell Host Microbe *13*, 701–710.

Samuelsson, C., Hausmann, J., Lauterbach, H., Schmidt, M., Akira, S., Wagner, H., Chaplin, P., Suter, M., O'Keeffe, M., and Hochrein, H. (2008). Survival of lethal poxvirus infection in mice depends on TLR9, and therapeutic vaccination provides protection. J. Clin. Invest. *118*, 1776–1784.

Schenten, D., and Medzhitov, R. (2011). The control of adaptive immune responses by the innate immune system. Adv. Immunol. *109*, 87–124.

Seiler, P., Aichele, P., Odermatt, B., Hengartner, H., Zinkernagel, R.M., and Schwendener, R.A. (1997). Crucial role of marginal zone macrophages and marginal zone metallophils in the clearance of lymphocytic choriomeningitis virus infection. Eur. J. Immunol. *27*, 2626–2633.

Sigal, L.J., Crotty, S., Andino, R., and Rock, K.L. (1999). Cytotoxic T-cell immunity to virus-infected non-haematopoietic cells requires presentation of exogenous antigen. Nature *398*, 77–80.

Sutherland, D.B., Ranasinghe, C., Regner, M., Phipps, S., Matthaei, K.I., Day, S.L., and Ramshaw, I.A. (2011). Evaluating vaccinia virus cytokine co-expression in TLR GKO mice. Immunol. Cell Biol. *89*, 706–715.

Swiecki, M., and Colonna, M. (2010). Unraveling the functions of plasmacytoid dendritic cells during viral infections, autoimmunity, and tolerance. Immunol. Rev. *234*, 142–162.

Swiecki, M., Wang, Y., Gilfillan, S., and Colonna, M. (2013). Plasmacytoid dendritic cells contribute to systemic but not local antiviral responses to HSV infections. PLoS Pathog. *9*, e1003728.

Tahiliani, V., Chaudhri, G., Eldi, P., and Karupiah, G. (2013). The orchestrated functions of innate leukocytes and T cell subsets contribute to humoral immunity, virus control, and recovery from secondary poxvirus challenge. J. Virol. *87*, 3852–3861.

Vabret, N., and Blander, J.M. (2013). Sensing microbial RNA in the cytosol. Front. Immunol. *4*, 468.

Van Rooijen, N. (1989). The liposome-mediated macrophage 'suicide' technique. J. Immunol. Methods *124*, 1–6.

Virgin, H.W. (2007). Pathogenesis of viral infection. In Fields' Virology, B.N. Fields, D.M. Knipe, and P.M. Howley, eds. (Philadelphia: Wolters Kluwer/Lippincott Williams & Wilkins), pp. 335–336.

Wang, X., Hussain, S., Wang, E.J., Wang, X., Li, M.O., García-Sastre, A., and Beg, A.A. (2007). Lack of essential role of NF-kappa B p50, RelA, and cRel subunits in virus-induced type 1 IFN expression. J. Immunol. *178*, 6770–6776.

Wu, J., and Chen, Z.J. (2014). Innate immune sensing and signaling of cytosolic nucleic acids. Annu. Rev. Immunol. *32*, 461–488.

Xu, R.H., Cohen, M., Tang, Y., Lazear, E., Whitbeck, J.C., Eisenberg, R.J., Cohen, G.H., and Sigal, L.J. (2008). The orthopoxvirus type I IFN binding protein is essential for virulence and an effective target for vaccination. J. Exp. Med. *205*, 981–992.

Xu, R.H., Remakus, S., Ma, X., Roscoe, F., and Sigal, L.J. (2010). Direct presentation is sufficient for an efficient anti-viral CD8+ T cell response. PLoS Pathog. *6*, e1000768.

Xu, R.H., Rubio, D., Roscoe, F., Krouse, T.E., Truckenmiller, M.E., Norbury, C.C., Hudson, P.N., Damon, I.K., Alcamí, A., and Sigal, L.J. (2012). Antibody inhibition of a viral type 1 interferon decoy receptor cures a viral disease by restoring interferon signaling in the liver. PLoS Pathog. *8*, e1002475.